

AD-A022 162

TUNABLE LASERS

C. Forbes Dewey, Jr., et al

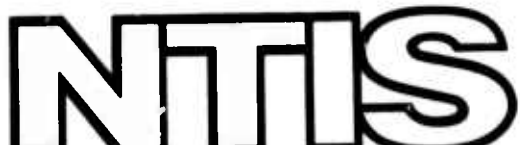
Massachusetts Institute of Technology

Prepared for:

Office of Naval Research

31 December 1975

DISTRIBUTED BY:



National Technical Information Service
U. S. DEPARTMENT OF COMMERCE

ADA022162

086142

SECURITY CLASSIFICATION OF THIS PAGE (When Data Entered)

REPORT DOCUMENTATION PAGE		READ INSTRUCTIONS BEFORE COMPLETING FORM
1. REPORT NUMBER FML-75-N2	2. GOVT ACCESSION NO.	3. RECIPIENT'S CATALOG NUMBER
4. TITLE (and Subtitle) Tunable Lasers - Semi Annual Technical Report #3		5. TYPE OF REPORT & PERIOD COVERED Technical 1 July 1975-31 December 1975
7. AUTHOR(s) C. Forbes Dewey, Jr. L. O. Hocker		6. PERFORMING ORG. REPORT NUMBER N00014-76-C-0431
9. PERFORMING ORGANIZATION NAME AND ADDRESS Massachusetts Institute of Technology 77 Massachusetts Avenue Cambridge, Massachusetts 02139		10. PROGRAM ELEMENT, PROJECT, TASK AREA & WORK UNIT NUMBERS
11. CONTROLLING OFFICE NAME AND ADDRESS Advanced Research Projects Agency 1400 Wilson Boulevard Arlington, Virginia 22209		12. REPORT DATE 31 December 1975
14. MONITORING AGENCY NAME & ADDRESS (if different from Controlling Office) Office of Naval Research Physics Program 800 North Quincy Street Arlington, Virginia 22217		13. NUMBER OF PAGES Unclassified
16. DISTRIBUTION STATEMENT (of this Report) Distribution is unlimited.		15. SECURITY CLASS. (of this report) 15a. DECLASSIFICATION/DOWNGRADING SCHEDULE
17. DISTRIBUTION STATEMENT (of the abstract entered in Block 20, if different from Report) DDC PROPRIETARY MAR 16 1976 REFUGEE C		
18. SUPPLEMENTARY NOTES		
19. KEY WORDS (Continue on reverse side if necessary and identify by block number) Nonlinear Optics, Lasers, Tunable Infrared, Proustite, Dye Laser		
20. ABSTRACT (Continue on reverse side if necessary and identify by block number) Tunable infrared radiation has been produced from 11μ to 23 by nonlinear mixing in proustite. Peak powers of 2 watts were shown for the wavelength range 16 to 20μ. Analysis of the data showed that a weak beam convergence at the crystal to be responsible for reduced power production at wavelengths where the crystal absorption was relatively weak. A theoretical study of this effect agrees well with the experiment.		
(continued on reverse side)		

(continued from front page)

20. Abstract

Specific applications for randomly twinned $\bar{4}3m$ crystals are shown. To form a proper theory for the development of such crystals we have studied the effects of crystal absorption and twin spacing on such crystals. We have also calculated the distribution function of the expected power from randomly twinned crystals and have shown it to take the form

$$w(P) = \frac{1}{N} e^{-P/N}$$

for large N.



Form Approved
Budget Bureau No. 22R0293

DEVELOPMENT OF POWERFUL WAVELENGTH-TUNABLE
INFRARED LASER SYSTEM

Technical Report No. 3

For Period Ending December 31, 1975

ARPA Order Number: 2840
Program Code Number: 6E20
Massachusetts Institute of Technology
Effective Date: July 1, 1975
Expiration Date: June 30, 1976
Total Value: \$44,987

Contract No.:
N00014-76-C-0431

Principal Investigator:
C. Forbes Dewey, Jr.
(617) 253-2235

Sponsored by Advanced Research Projects Agency ARPA Order No. 2840.

The views and conclusions contained in this document are those of the authors and should not be interpreted as necessarily representing the official policies, either expressed or implied, of the Advanced Research Projects Agency or the U. S. Government.

TUNABLE LASERS

ARPA Contract No. N00014-76-C-0431

Technical Report No. 3

For Period Ending 12/31/75

Summary

In our research on nonlinear crystals and processes for frequency mixing in the infrared we have made progress along two fronts.

We have produced tunable infrared from 11μ to 23μ by mixing the outputs from two ruby-pumped dye lasers in proustite. Peak powers of 2 watts were shown for the wavelength range $16-20\mu$. Analysis of the output power versus wavelength showed that beam convergence at the nonlinear crystal can be responsible for a substantial reduction in output from that which one would expect were the crystal at the beam waste. This effect is studied quantitatively and an excellent agreement is found between theory and experiment.

We show that there are applications where randomly twinned crystals could meet specific needs for crystals to be used in nonlinear mixing processes. In order to lay a proper background for the development of such crystals we have made a preliminary theoretical investigation of the effects of crystal absorption and twin spacing on the power production from a randomly twinned crystal. We have also found the probability distribution function for the power produced by a randomly twinned crystal. This distribution function has the form

$$w(P) = \frac{1}{N} e^{-P/N}$$

where N is the number of twins with spacings larger than the coherence length, and $N \gg 1$. P is normalized so that N twin planes give on the average a power of N . Since the distribution is quite wide there is a substantial probability of getting much less power than expected. The probability of observing an enhancement of $N/2$ or less for N twins is 40%. Accordingly some crystal selection will be necessary.

DEVELOPMENT OF POWERFUL WAVELENGTH-TUNABLE
INFRARED LASER SYSTEM

ARPA Contract No. N0001-76-C-0431

Semi-Annual Technical Report No. 3

For Period Ending December 31, 1975

Research Program:

In our research program we have been studying in detail, various approaches to the production of tunable infrared power. The emphasis of this program lies with nonlinear mixing in solids. In this vein we are studying traditional phase matchable materials and also materials that are not traditionally phase matchable but are potentially so given the development of techniques to produce controlled twinning. Raman shifting of dye laser radiation to produce tunable I.R. has great potential. We are not currently pressing this program.

Accomplishments:

A) Phase Matchable Materials. We have studied difference frequency generation in proustite in a frequency range where the crystal shows substantial absorption. The variation of the absorption coefficient with wavelength was used to probe the effective coherence length of the mixing process and show that even a weak beam convergence or divergence at the crystal can produce a substantial reduction in the difference frequency power from that which one would expect were the crystal at the beam waist.

This work is being written for publication and a draft of this paper appears as Appendix I.

B) Phase Matching by Twin Planes. The coherence length for some nonlinear mixing processes in $\bar{4}3m$ materials can be fairly long. For example the coherence length for frequency doubling of 10.6μ radiation is greater than 200μ for both CdTe and ZnTe. This combination of large coherence length, large nonlinear coefficient and high damage threshold means that it is practical to consider synthesizing a crystal from a stack of carefully cut and polished plates, each with a precise orientation and thickness. A relatively few plates (5 or 6) is quite sufficient to cause pump depletion. Such an experiment is currently in progress at Los Alamos using CdTe. In order to assure some strength these plates were cut and polished to a thickness several times the coherence length. The orienting, cutting, and polishing requirements are quite stringent as each plate must be oriented so that both the fundamental and the harmonic beam have the same polarization and can enter and leave the crystals at Brewster's angle. The optical path length inside the crystal must also be very close to $n + 1/2$ coherence lengths so that the cumulative errors of several plates will not be important.

It occurred to us that the same result could be achieved much more readily by using a randomly twinned crystal with 30 or more twins spaced by at least 200μ . This crystal would have approximately the same thickness as the synthesized crystal but would not have the same orientation

requirements. It would also have only two surfaces, neither one critical. The power produced by the stack of plates is proportional to the square of the number of plates (ignoring depletion) while for randomly spacing we expect a linear relationship between the number of twins and the power produced. Accordingly 30 randomly spaced twins would produce as much harmonic power as 5 or 6 plates.

Since for such applications randomly twinned crystals appear to have considerable potential we have considered randomly twinned crystals from a theoretical standpoint. Appendices II, III, and IV study briefly three different aspects of this problem.

APPENDIX I

DIFFERENCE FREQUENCY GENERATION IN PROUSTITE FROM 11 TO 23 μ

Proustite has been shown to be a useful nonlinear material by a multiplicity of authors. Harmonic⁽¹⁾ and difference-frequency generation,^(2,3,4) parametric oscillation,^(5,6) and up conversion^(7,8,9) have been successfully accomplished over the wavelength range of about 1 to 12 μ . The high intrinsic absorptivity of this material for wavelengths greater than 12 μ , however, has provided a deterrent for nonlinear mixing experiments at these longer wavelengths. In this experiment we have used difference-frequency generation in proustite to produce tunable I.R. over the wavelength range 11 to 23 μ . Despite substantial absorption, significant levels of I.R. power are achieved over most of this wavelength range.

A ruby laser was used to end pump two tunable dye lasers operating with orthogonal polarizations. These two lasers operated in the wavelength range .84 + 1.0 μ using Kodak dye Air 1 and Nippon Kankoh-Shikiso Kenkyusho dye NK 1748. The dye laser outputs were about 5 mJ with a pulse width of about 30 ns. The linewidths were measured to be about 3 \AA . By mixing the output of these two dye lasers the entire range of 11 to 23 μ could be phase matched with only a 7 $^{\circ}$ rotation of the proustite crystal. The phase matching angles were found to be close to those calculated from the index of refraction data of Hobden⁽¹⁰⁾. In order to

correlate the generated infrared power with the absorptivity of proustite it was necessary to measure the absorption coefficient of proustite over the wavelength range of interest. Previous measurements of the proustite absorption coefficient in this wavelength range^(11,12,13) were not sufficiently quantitative for our purposes. Proustite is a negatively birefringent uniaxial crystal, and type 1 phase matching was used. The I.R. signal exists in the crystal as an ordinary wave; accordingly, we measured the ordinary wave absorption coefficient. This measurement was performed on a Beckman IR-12 dual-beam spectrophotometer operated in the single beam mode. Polarization was provided by an AgCl polarizer. Transmission measurements were made on crystals⁽¹⁴⁾ (grown, cut and polished by R.R.E) with thicknesses of 3 mm, 1.0 mm and 0.3 mm. The results of these measurements are shown on Figure 1.

The absorption peaks at 10μ , 14.5μ , 16.5μ and 22.5μ are readily identifiable as combination and overtone bands by reference to the comprehensive work⁽¹⁵⁾ of Byer, Bobb, Lefkowitz and Deaver. Their notation is used in the absorption peak identifications shown in Fig. 1.

Measurements were made of the infrared power generated by mixing the outputs of the two ruby-pumped dye lasers in a 4 mm thick proustite crystal⁽¹⁴⁾. The crystal was cut 20° to the optic axis in the appropriate quadrant to make the d_{31} and d_{22} contributions to the nonlinear polarizations additive⁽¹⁶⁾. For each wavelength the crystal orientation was adjusted for optimum output. Focusing of the dye laser beams was accomplished with a 35 cm focal length lens. A f:2 mirror was used to focus the infrared radiation leaving the crystal onto HgCdTe detector.

The results of these measurements are shown on Fig. 1. The responsivity of the HgCdTe detector used for these measurements peaked at about 17μ and fell off rapidly at longer wavelengths. The exact shape of the detector response curve is of considerable importance for determining the power levels reached for wavelengths greater than 17μ .

A twinned ZnSe crystal⁽¹⁷⁾ was used in place of the proustite to calibrate the detector. This crystal is transparent out to about 22μ . Past 17μ the detected signal was observed to chop off at between a factor of 2.4 and 2.8 per micron. Correcting for the expected λ^2 dependence of the difference frequency generation, and adding an additional factor of λ to compensate for the reduced number of twins available at longer wavelengths we find the detector fall off to be between 2.0 and 2.4 per micron. We have adopted the factor of 2 fall off rate for these measurements as it seems to describe the data most consistently.

In order to see the influence of absorption on the infrared power produced in the experiment we must first remove the wavelength dependence. Besides the explicit λ_{IR}^{-2} power dependence the variation of the indices of refraction and nonlinear coefficient with wavelength must be considered. The refractive index variations are small for the difference frequency wavelength range $10 \rightarrow 24\mu$ both for the IR beam and the pump beams. This implies by Miller's rule⁽¹⁸⁾ that the nonlinear coefficient will also change only slightly. We consider these wavelengths too far removed from restrahl for resonance effects such as those seen by Faust and Henry⁽¹⁹⁾ to be important. Thus to some reasonable approximation the wavelength dependence only as the usual λ^{-2} term and indirectly

through the absorption coefficient. Thus we find

$$P\lambda^2 = A L_{\text{eff}}^2(\alpha) \quad (1)$$

where L_{eff} is the effective crystal length taking into account absorption, beam walk off and the like. Figure 2 shows L_{eff}^2 , suitably normalized, plotted against the absorption coefficient α data at all wavelengths we measured. (The normalization of L_{eff}^2 will be apparent later.) Since this plot combines the experimental errors of both the absorption coefficient and I.R. difference frequency experiments, it is not surprising that there is substantial scatter in the data.

The effective length of an absorbing crystal used in a difference frequency generation experiment can be readily derived. Following the approach of Miller and Nordland⁽¹⁸⁾ we find for perfect phase matching

$$\left(\frac{L_{\text{eff}}}{L}\right)^2 = \frac{1 + e^{-\alpha L} - 2e^{-1/2 \alpha L}}{\left(\alpha/2\right)^2} \quad (2)$$

It is not possible to fit the observed data with this function.

This equation appears as the $\Delta K = 0$ curve on Figure 2. The only free parameter in this equation is the normalization which corresponds to an arbitrary displacement of the curve along the vertical axis. It is clear that if the curve is forced to fit the data for large α it will not fit for small α and vice versa. In the limit of strong absorption, we expect an $1/\alpha^2$ dependence of the power regardless of other effects,

and accordingly it is appropriate to match equation (2) to the large α points. The discrepancy between the observed and expected values for small α must be due to a limitation other than crystal length.

Double refraction and beam divergence⁽²⁰⁾ are not to blame, as for this experiment both the aperture length and the effective length of focus were substantially greater than the crystal length. Nor is it possible that the dye laser linewidths are responsible, as they are only about 4 cm^{-1} , and the phase matching angle varies only very slowly with wavelength. (Indeed at 18μ this change is zero.) However the crystal was not placed at the focus of the lens, and accordingly the crystal spread meant that all parts of the input beams could not be phase matched for the same crystal orientation. This effect was responsible for the early saturation of the power production.

In order to determine quantitatively the effect of this spread of input angles we must return to a more general form of equation 2, leaving in the effect of imperfect phase matching and integrating over a distribution of input angles.

$$\left(\frac{L_{\text{eff}}}{L}\right)^2 = \frac{S}{\int I_1(\theta, \phi) I_2(\theta, \phi) d\theta d\phi} \frac{\int \frac{(1 + e^{-\alpha L} - 2e^{-1/2\alpha L} \cos(\Delta K(\theta, \phi)L)}{(\Delta K(\theta, \phi)L)^2 + (\alpha L/2)^2} I_1(\theta, \phi) I_2(\theta, \phi) d\theta d\phi}{\int I_1(\theta, \phi) I_2(\theta, \phi) d\theta d\phi} \quad (3)$$

Here $I_1(\theta, \phi)$, $I_2(\theta, \phi)$ are the intensity distribution of the point beams and $\Delta K(\theta, \phi) = 2\pi \left(\frac{n_1(\theta, \phi)}{\lambda_1} - \frac{n_2}{\lambda_1} - \frac{n_3}{\lambda_1} \right)$. We have assumed that the

crystal is far from the focal point of the lens so that $I_1(\theta, \phi)$ and $I_2(\theta, \phi)$ are essentially constant over the length of the crystal.

This integration is not possible to do analytically in general, but can be approximated after some simplifying assumptions are made. First, we assume $I_1(\theta, \phi)$ and $I_2(\theta, \phi)$ are rectangular functions with the same width. This is a good approximation for our case as the dye lasers were run multimode and apertured outside the cavity. Secondly, we consider the distribution of input angles to be the same for both dye beams, appropriate for our case, but not in general as often lenses are used to match beam sizes and are accordingly only used in one beam^(2,4). Since the outputs of the two dye lasers employed in our experiment had nearly identical spatial characteristics, the lens was used to adjust the power density at the crystal. For the phase matching angle used in this experiment, the angular spread in the plane of the optic axis contributed much more to the mismatch than the spread perpendicular to it and we can ignore the contribution due to the beam spread perpendicular to the optic axis.

After defining the full width of the rectangular functions $I_n(\theta, \phi)$ as a ; and defining $g = \frac{d(\Delta K)}{d\theta}$ we can look at this equation in a few of its limits:

- 1) for $aL \gg 1$, $aL \gg gaL$ $\left(\frac{L_{\text{eff}}}{L}\right)^2 \rightarrow \frac{4}{(aL)^2}$
- 2) for $gaL \ll 1$, $aL \ll 1$ $\left(\frac{L_{\text{eff}}}{L}\right)^2 \rightarrow 1$
- 3) for $aL \ll 1$, $gaL \gg 1$ $\left(\frac{L_{\text{eff}}}{L}\right)^2 \rightarrow \frac{2\pi}{gaL}$

Intermediate values can be obtained by machine integration. Where great accuracy is not required the approximation of the integration for $gaL \gg 1$ is given by

$$\left(\frac{L_{\text{eff}}}{L}\right)^2 \sim \frac{4}{\alpha g a L^2} \left(1 - e^{-\alpha L/2}\right) \left[\left(1 - e^{-\alpha L/2}\right) \tan^{-1} \frac{g a L}{\alpha L} + \pi e^{-1/2 \alpha L} \right] \quad (4)$$

This equation is plotted in figure 2 for various values of gaL . Best fit to the data is found with $gaL = 20$. This is in reasonable agreement with experiment as $ga \approx 40 \text{ cm}^{-1}$ for our experiment and $L = .4 \text{ cm}$ giving an anticipated value of gaL of 16.

In conclusion we have shown that reasonable levels of tunable infrared power can be produced in crystals that show strong absorption. In assessing the value of a nonlinear crystal, it is apparent that such terms as transparent and opaque should be used with caution. We have also shown the effect of a spread of beam angles on the power produced in a nonlinear crystal. Even a weak beam convergence can lead to a substantial reduction in the difference frequency power generated.

References

1. D. M. Boggett and A. F. Gibson, Physics Letters 28A, 33 (1968).
2. D. C. Hanna, R. C. Smith and C. R. Stanley, Optics Communications 4, 300 (1971).
3. G. C. Bhar, D. C. Hanna, B. Luther-Davies and R. C. Smith, Optics Communications 6, 323 (1972).
4. C. D. Decker and F. K. Tittel, Appl. Phys. Lett. 22, 411 (1973).
5. E. O. Ammann and M. M. Yarborough, Appl. Phys. Lett. 17, 233 (1970).
6. D. C. Hanna, B. Luther-Davies, and R. C. Smith, Appl. Phys. Lett. 22, 440 (1973).
7. J. Warner, Appl. Phys. Lett. 12, 222 (1968).
8. J. Warner, Appl. Phys. Lett. 13, 360 (1968).
9. E. K. Pfitzer, H. D. Ruccins and K. J. Siemsen, Optics Communications 3, 277 (1971).
10. M. V. Hobden, Opto-Electronics 1, 159 (1969).
11. L. Guseva, I. G. Gameev, A. V. Dronov and I. S. Rez, Optiki i Spektroskopiia 24, 298 (1968).
12. Ya. O. Dovgii, V. N. Korolyshin, E. G. Moroz, and V. V. Turkevich, Optiki i Spektroskopiia 31, 307 (1971).
13. Ya. O. Dovgii, N. I. Butsko, V. N. Kordyshin, and E. G. Moroz, Soviet Physics-Solid State 13, 995 (1971).
14. The crystals used in absorption measurements were grown, oriented, cut, and polished by the Royal Radar Establishment (RRE), Malvern, England. Difference-frequency generation was accomplished in RRE crystals cut and polished by Mann Labs., Cambridge, Ma.

15. H. H. Byer, L. C. Bobb, I. Lefkowitz and B. S. Deaver, Ferroelectrics 5, 207 (1973).
16. K. F. Hulme, O. Jones, P. H. Davies, and M. V. Hobden, Appl. Phys. Lett. 10, 133 (1967).
17. C. F. Deway, Jr. and L. O. Hocker, Appl. Phys. Lett. 26, 442 (1975).
18. R. C. Miller and W. A. Nordland, Phys. Rev. B2, 4896 (1970).
19. W. L. Faust and C. H. Henry, Phys. Rev. Lett. 17, 1265 (1966).
20. G. D. Boyd and D. A. Kleinman, J. Appl. Phys. 39, 3597 (1968).

Fig 1.

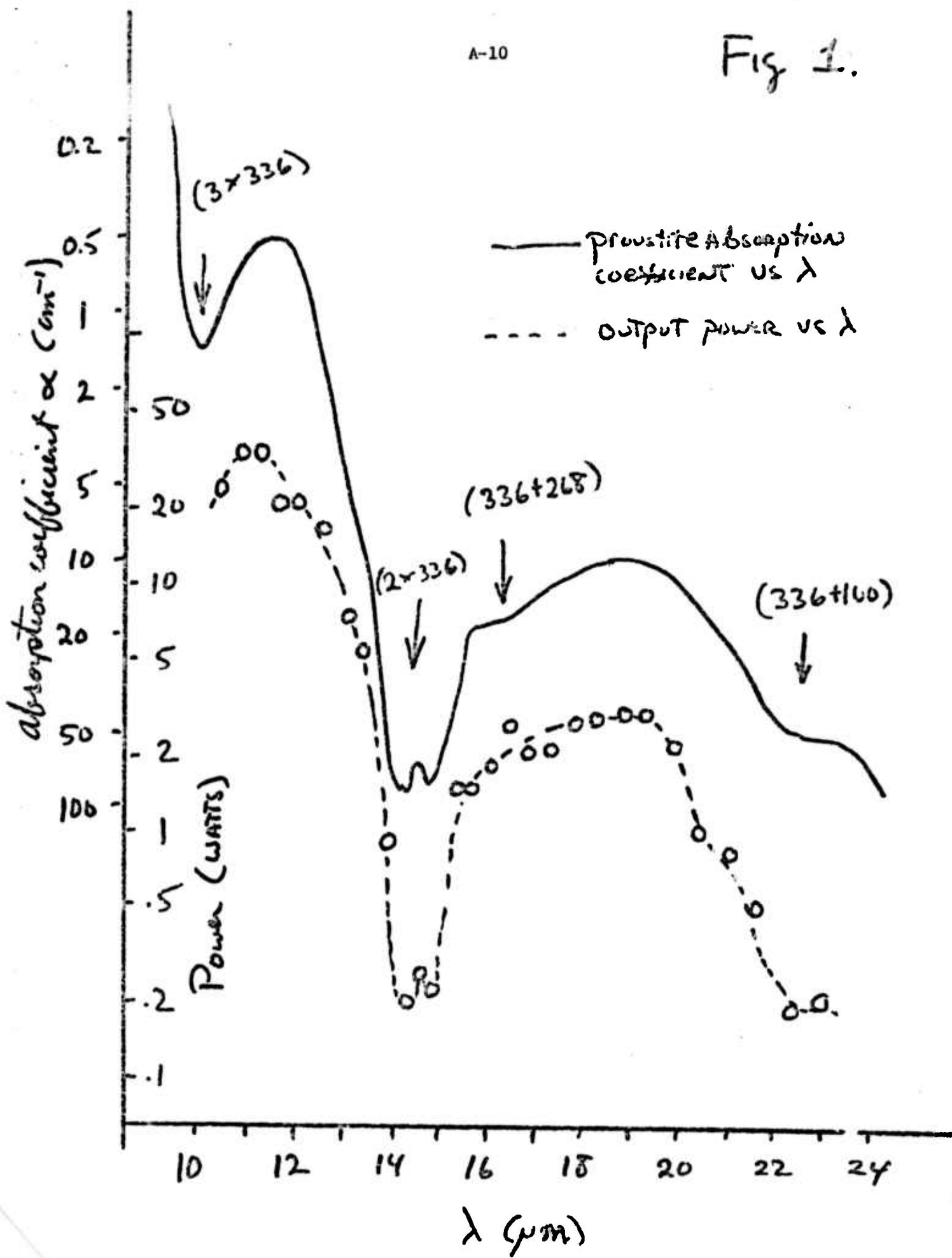
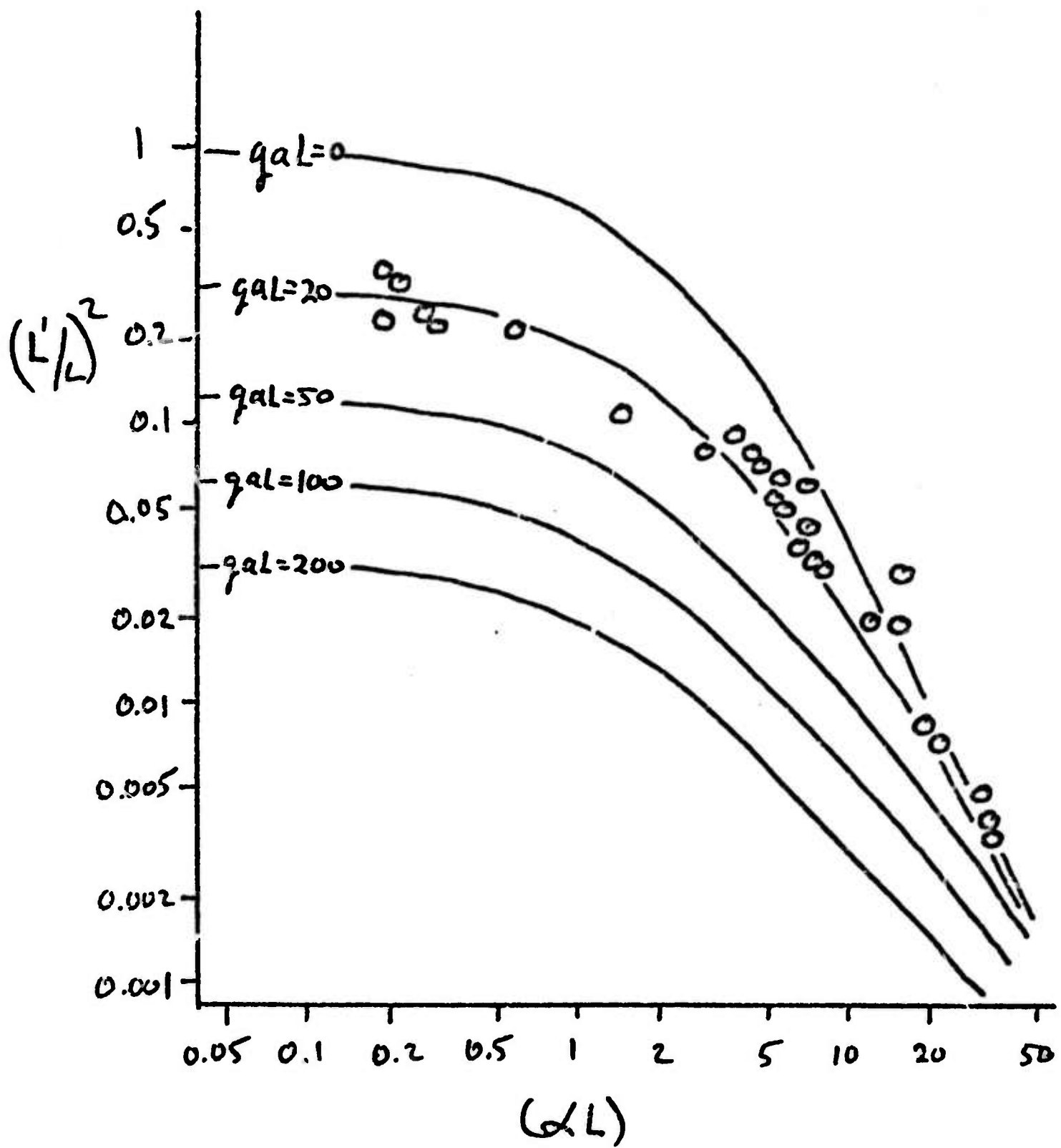


Fig 2



APPENDIX II

POWER PRODUCED BY HARMONIC GENERATION IN A RANDOMLY TWINNED ABSORBING CRYSTAL

We show here a derivation of equation (1) given without proof in our paper Enhancement of Second-Harmonic Generation in Zinc Selenide by Crystal Defects.

We chose as a comfortable starting point equation 2.41 (page 43) of Zernike and Midwinter's book Applied Nonlinear Optics.

For general $\omega_1 + \omega_2 = \omega_3$ mixing

$$E_3 = \frac{-8\pi i \omega_3^2 d_{123}}{K_3 c^2} E_1 E_2 \int_0^L e^{i\Delta Kz} dz \quad (1)$$

In the special case of frequency doubling $E_1 = E_2$. Also

$$\Delta K = 2\pi \left(\frac{2n_1}{\lambda_1} - \frac{n_3}{\lambda_3} \right) = \frac{4\pi(n_1 - n_3)}{\lambda_1}$$

where the subscript 1 refers to the fundamental and 3 to the harmonic.

Thus

$$E_3 = \frac{-8\pi i \omega_3^2 d_{113}}{K_3 c^2} E_1^2 \int_0^L e^{i\Delta Kz} dz \quad (2)$$

With N twins, the crystal is broken into $N + 1$ domains with a reversal of sign of the nonlinear coefficient in each domain. If the twins appear at positions L_j

$$\begin{aligned}
 E_3 &= \frac{-8\pi i \omega_3^2 d_{113}}{K_3 c^2} E_1^2 \sum_{j=0}^N (-1)^j \int_{L_j}^{L_{j+1}} e^{i\Delta K z} dz \\
 &= \frac{-8\pi i \omega_3^2 d_{113}}{K_3 c^2} E_1^2 \sum_{j=0}^N (-1)^j \frac{1}{i\Delta K} \left[e^{i\Delta K L_{j+1}} - e^{i\Delta K L_j} \right] \quad (3) \\
 &= \frac{-8\pi i \omega_3^2 d_{113}}{K_3 c^2 \Delta K} E_1^2 \left[2 \sum_{j=1}^N (-1)^j e^{i\Delta K L_j} + e^{i\Delta K L_0} + (-1)^{N+1} e^{i\Delta K L_{N+L}} \right]
 \end{aligned}$$

R. C. Miller and W. A. Nordland [Phys. Rev., B2, 4896, (1970)] show how to account for absorption:

$$n = n' + \frac{i\lambda_3 \alpha_3}{4\pi} \quad (4)$$

so

$$\frac{\Delta K}{2\pi} = \frac{2n_1}{\lambda_1} - \frac{n'_3}{\lambda_3} - \frac{i\lambda_3 \alpha_3}{\lambda_3 4\pi} = \frac{\Delta K'}{2\pi} - \frac{i\alpha_3}{4\pi} \quad (5)$$

Here the primed n and K are pure real. Substituting we find:^{*}

$$E_3 = \frac{-8\pi \omega_3^2}{K_3 c^2} \frac{d_{113} E_1^2}{(\Delta K - i\alpha/2)} \left[(-1)^{N+1} + 2 \sum_{j=1}^N (-1)^j e^{\alpha/2 L_j} e^{i\Delta K' L_j} \right] \quad (6)$$

so

^{*} L_{N+1} corresponds to the far edge of the crystal so $L_{N+1} = 0$ and $L_0 = -L$ where L is the crystal length. Assume a large number of twins with $\Delta K \gg 1$.

$$\begin{aligned}
 P_3 &= \frac{cn_3}{2\pi} E_3 E_3^* = \frac{64 \pi^2 \omega_3^4 n_3 d_{113}^2 (E_1 E_1^*)^2}{2\pi K_3^2 c^3 (\Delta K'^2 + \alpha^2/4)} \\
 &\cdot \left[1 + 2 \sum_{j=1}^N e^{-\alpha/2 L_j} \left(e^{+i\Delta K' L_j} + e^{-i\Delta K' L_j} \right) (-1)^{N+j+1} \right. \\
 &\left. + 4 \sum_{j=1}^N \sum_{k=1}^N (-1)^{j+k} e^{-\alpha/2(L_j + L_k)} e^{i\Delta K'(L_j - L_k)} \right] \quad (7)
 \end{aligned}$$

Obviously (7) is of little help when we don't know the values of the L_j , but if we assume they are randomly spaced everything simplifies greatly. For close twin spacings $2\pi \gg (\Delta K(L_j - L_{j+1}))$ the second term contributes nothing as it alternates sign with each twin while the cosine term changes only slightly. For wide twin spacings $\Delta K(L_j - L_{j+1}) > 2\pi$ the cosine term has essentially randomized by the next plane so for randomly spaced twins this term will contribute nothing. The third term will suffer the same cancellations except for the cases $j = k$. So under this assumption

$$P_3 = \frac{32 \pi \omega_3^2 n_3 d_{113}^2 (E_1 E_1^*)^2}{(n_3)^2 \omega_3^2 c (\Delta K'^2 + \alpha^2/4)} \left[1 + 4 \sum_{j=1}^N e^{-\alpha L_j} \right] \quad (8)$$

If we assume the twins are roughly evenly distributed through the crystal, then the sum can be replaced by an integral for large N

$$\sum_{j=1}^N e^{-\alpha L_j} + \frac{N}{L} \int_0^L e^{-\alpha x} dx = \frac{N}{\alpha L} (1 - e^{-\alpha L}) \quad (9)$$

So

$$P_3 = 32\pi \frac{c}{\lambda_3^2 n_3} d_{113}^2 \frac{p_1^2 4\pi^2}{\Delta K^2 + \alpha^2/4} \left[\frac{1 + \frac{4N}{\alpha L} (1 - e^{-\alpha L})}{\Delta K^2 + \alpha^2/4} \right] \quad (10)$$

But by Miller's rule

$$d_{113} = (n_1^2 - 1)^2 (n_3^2 - 1) \delta_{113}$$

where δ_{113} is a material constant independent of the index (Miller's δ). So

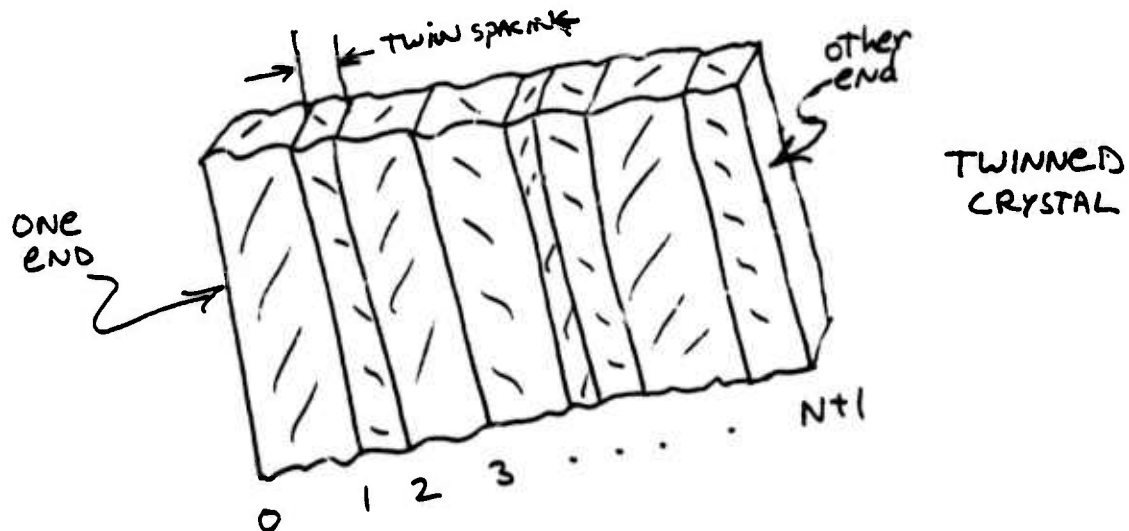
$$P_3 = \frac{128\pi^3 p_1^2 (n_1^2 - 1)^4 (n_3^2 - 1)^2 \delta_{113}^2}{\lambda^2 n_3 n_1^2 c} \left[\frac{1 + \frac{4N}{\alpha L} (1 - e^{-\alpha L})}{\Delta K^2 + \alpha^2/4} \right] \quad (11)$$

The key approximation appears in the step between equations 7 and 8. The assumption there is that the phases of the radiation emitted by each segment are randomly correlated. In practice there is some accidental correlation which brings in contributions from those terms. Recently we took one crystal orientation and swept ΔK (by changing λ) and observed large fluctuations in the power produced in a difference frequency measurement. This modulation results from the changing contributions from these terms (which can subtract from the power produced as well as add to it). Periodic twinning with the right spacing would produce positive contributions from all these terms.

APPENDIX III

DIFFERENCE FREQUENCY POWER PRODUCED BY N TWINS WITH AN ARBITRARY SPACING IN A NON-ABSORBING $\bar{4}3m$ CRYSTAL

In this model we consider a crystal with N twin planes separated by distances large compared to a coherence length.



For simplicity we will assume $N \gg 1$ so we can ignore contributions from the ends. We also consider $\alpha L \ll 1$ so that absorption effects are negligible. In this case for difference frequency generation

$$P_3 = \frac{128 \pi^3 d_{123}^2 P_1 P_2}{\lambda_3^2 n_3 n_2 n_1 c(\Delta k')^2} \left[4 \sum_{j=1}^N \sum_{k=1}^N (-1)^{j+k} e^{i \Delta k' (L_j - L_k)} \right]. \quad (1)$$

This equation follows from equation (7) in Appendix II.

We break down this equation to see separately the contributions from the $j = k$ and the $j + k$ terms

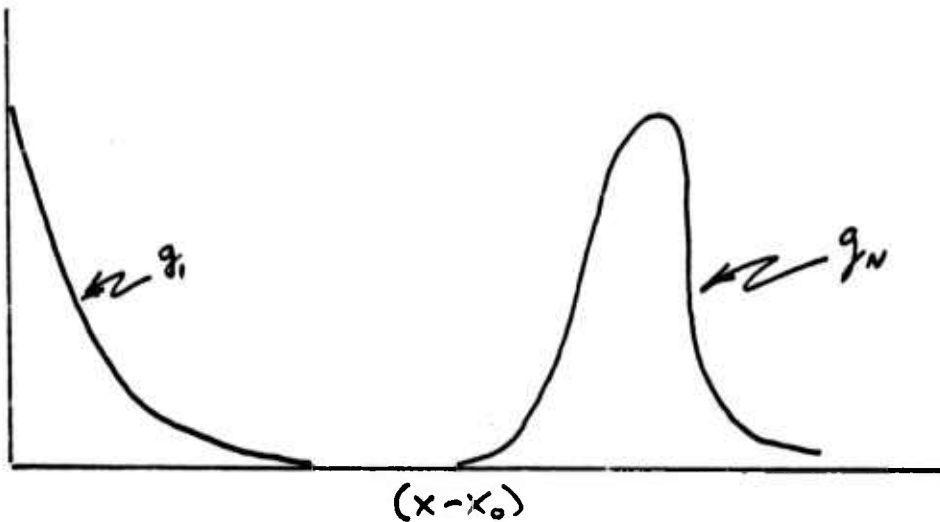
$$P_3 \propto N + \sum_{j=1}^{N-1} \sum_{k=j+1}^N (-1)^{j+k} \left(e^{i\Delta K'(L_j - L_k)} + e^{-i\Delta K'(L_j - L_k)} \right)$$

$$= N + 2 \sum_{j=1}^{N-1} \sum_{k=j+1}^N (-1)^{j+k} \cos[\Delta K'(L_j - L_k)] \quad (2)$$

A simplest model of the twin spacing would evoke a function $g_1(x-x_0)$ which is defined as the probability of finding the next twin at position x , given a twin at position x_0 . We assume here that a twin's positional probability can be written as a function of the position of the previous twin without explicit dependence on the position of the twin before that one, and also that knowledge of the positions of all previous twins will provide no further information. This is a very powerful assumption and probably is not generally the case. Given that assumption we can proceed to find $g_n(x-x_0)$, the probability of finding at x the n^{th} twin away from the twin at x_0 .

$$g_n(x-x_0) = \int_{x_0}^x g_1(x'-x_0) g_1(x-x') dx' \quad (3)$$

$$g_n(x-x_0) = \int_{x_0}^x g_{n-1}(x'-x_0) g_1(x-x') dx' \quad (4)$$



We return to equation (2) for a moment and rewrite it by twin spacings

$$P_3 \approx N + \sum_{j=1}^{N-1} \sum_{k=1}^{N-j} (-1)^k \cos \Delta K (L_j - L_{j+k}) \quad (5)$$

and

$$P_3 \approx N + 2 \sum_{k=1}^{N-1} \sum_{j=1}^{N-k} (-1)^k \cos \Delta K (L_j - L_{j+k}) \quad (6)$$

Now we average over the probability distributions to get the average power.

$$P_3 \approx N + 2 \sum_{k=1}^{N-1} (N-k) (-1)^k \int_0^{\infty} \cos \Delta K g_k(x) dx \quad (7)$$

Consider first the case where the coherence length is very long or $g_k(x)$ has very small values. In this limit

$$\int_0^{\infty} \cos \Delta K g_k(x) dx \rightarrow 1$$

and

$$P_3 = N + 2 \sum_{k=1}^{N-1} (N-k) (-1)^k$$

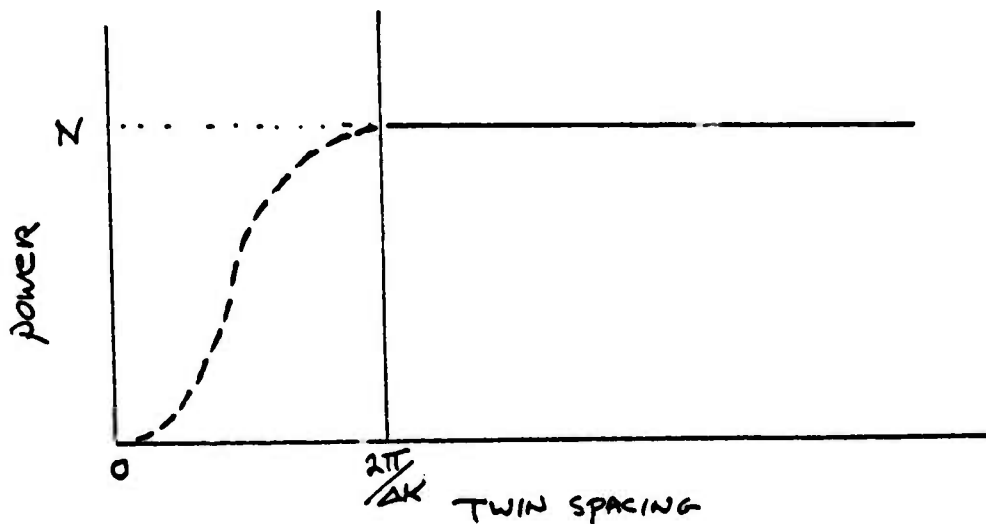
$$= \begin{cases} 0 & (\text{for } N \text{ odd}) \\ 1 & (\text{for } N \text{ even}) \end{cases} \quad (8)$$

Thus very closely spaced twins do not contribute to the radiated power.

If we make the opposite assumption (as in Appendix II) and $\Delta K g_k(x) \gg 2\pi$, then the cosine terms average to zero and

$$P_3 \approx N \quad (9)$$

We find then that the power radiated from a group of N twins randomly spaced but with a characteristic spacing ΔL goes roughly

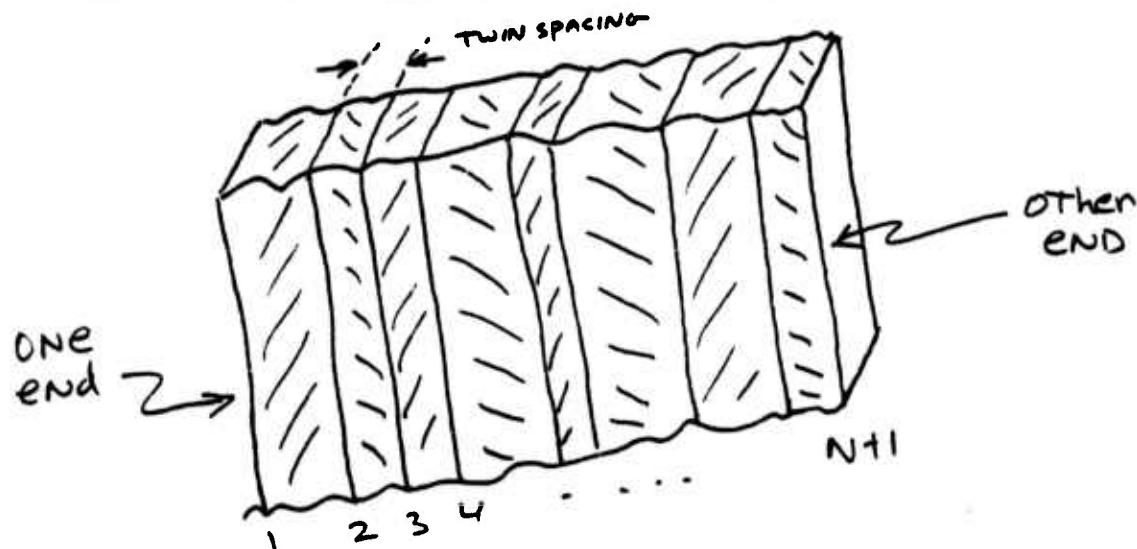


An accurate description of the region between 0 and $2\pi/\Delta K$ would require accurate knowledge of the $g_k(x)$.

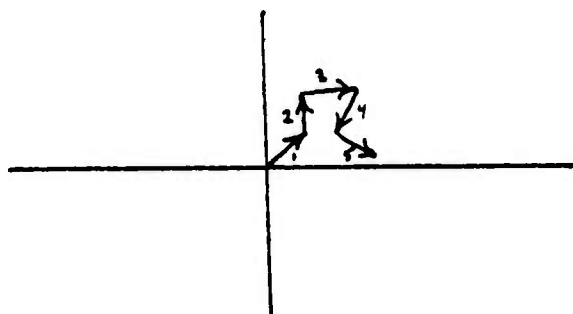
APPENDIX IV

DISTRIBUTION OF OUTPUT POWERS OF A RANDOMLY TWINNED NON ABSORBING CRYSTAL WHERE THE COHERENCE LENGTH IS MUCH SMALLER THAN THE TWIN SPACING

In this model we consider a crystal with N twin planes separated by distances large compared to a coherence length.



For simplicity we assume $N \gg 1$ so we can ignore the contributions from the ends. We also consider $\alpha L \ll 1$ so that absorption effects are negligible. In this case the radiation E fields effectively produced at each twin site add up as in a random walk.



The probability distribution of the end point $\omega(\vec{E})$ is determined by this two dimensional random walk.

$$\omega(\vec{E}) = \frac{1}{\pi N} e^{-|\vec{E}|^2/N} \quad (1)$$

Here we have chosen the normalization so that the field produced for each twin is of unit value.

The distribution is radially symmetric so we can convert from \vec{E} to E magnitude easily

$$\omega(E) = \int_0^{2\pi} \omega(\vec{E}) d\theta = \frac{2}{N} e^{-E^2/N} \quad (2)$$

We can check what the average power we can expect is by solving

$$\overline{E^2} = \int_0^{\infty} E^2 \omega(E) EdE = \frac{2}{N} \int_0^{\infty} E^2 e^{-E^2/N} EdE \quad (3)$$

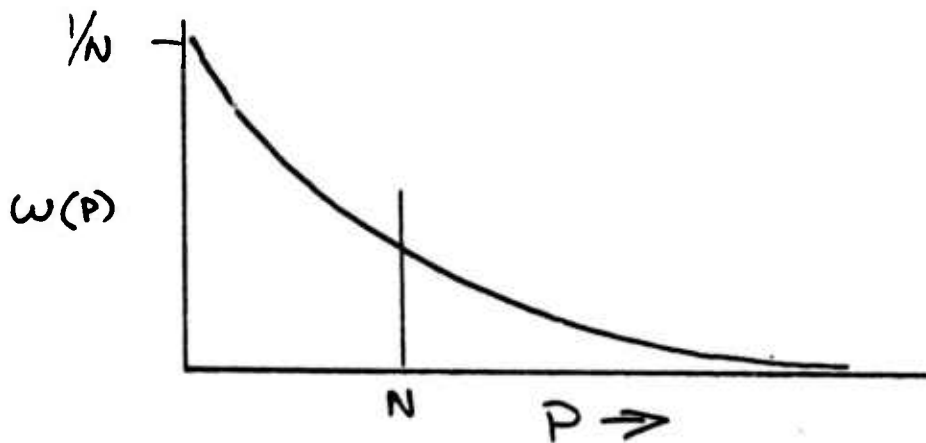
For clarity we substitute $P = E^2$, $dP = 2EdE$ so

$$\overline{P} = \overline{E^2} = \frac{1}{N} \int_0^{\infty} Pe^{-P/N} dP = N \quad (4)$$

which is as we expected.

We also have found the probability distribution function for P

$$\omega(P) = \frac{1}{N} e^{-P/N} \quad (5)$$



In many practical experimental situations, a spread of convergence angles, local spatial heating and spreads of input wavelengths will mean that a number of different samples of this distribution will be made for each pulse. Effectively, different parts of the beam will see different sets of spacings of the twins. As has been done in other branches of physics we shall loosely define a term "coherence area" to refer to that part of the beam that sees the same set of twin spacings. For the next section we will consider the case of there being m such coherence areas each sharing the same fraction of the input beam.

To develop the function $\omega(P,m)$ we shall first find $\omega(P,2)$

$$\begin{aligned}
 \omega(P,2) &= \int_0^P \omega(P') \omega(P-P') dP' \\
 &= \int_0^P \frac{1}{N^2} e^{-P'/N} e^{-(P-P')/N} dP' = \frac{P}{N^2} e^{-P/N} \quad (6)
 \end{aligned}$$

Continuing,

$$\begin{aligned}\omega(P, 3) &= \int \omega(2P', 2) \omega(P-P') dP' \\ &= \int \frac{1}{N^3} P' e^{-P'/N} e^{-(P-P')/N} dP' = \frac{1}{2} \left(\frac{P}{N}\right)^2 \frac{e^{-P/N}}{N} \quad (7)\end{aligned}$$

By now the limit is clear

$$\omega(P, m) = \frac{1}{m!} \left(\frac{P}{N}\right)^m \frac{e^{-P/N}}{N} \quad (8)$$

This has the form of a poissonian distribution

$$P = \frac{e^{-b} b^a}{a!} \quad (9)$$

which has, in the limit of large b, the form

$$P \rightarrow \frac{1}{\sqrt{2\pi b}} e^{-(a-b)^2/2b} \quad (10)$$

Accordingly we find

$$\omega(P, m) \rightarrow \frac{1}{N} \frac{1}{\sqrt{P/N}} e^{-(m-P/N)^2/2P/N} \quad (11)$$

for large m.

We have now m times as great an average power, as m different systems were added together. In reality each of these systems had $1/m$ of the input power so we must substitute mP for P .

$$\omega(P, m) = \frac{1}{\sqrt{NPm}} e^{-(m-mP/N)^2/2P/N} \quad (12)$$

$$= \frac{1}{\sqrt{NPm}} e^{-(P-N)^2/2PN/m} \quad (13)$$

For large m (already assumed in (11)) this becomes

$$\omega(P, m) \approx \frac{1}{\sqrt{NPm}} e^{-(P/N)^2/2N^2/m} \quad (14)$$

which has a half width of N/\sqrt{m} .

To find a r.m.s. fluctuation of a factor of two one would therefore need

$$.3N = N/\sqrt{m}$$

so

$$m \sim 10$$

APPENDIX V

BIBLIOGRAPHY OF PAPERS RELATED TO ENHANCED NONLINEAR OPTICAL EFFECTS IN ROTATIONALLY TWINNED CRYSTALS

C. F. Dewey, Jr.
L. O. Hocker

A. Nonlinear Effects in Rotationally Twinned Crystals

1. C. F. Dewey, Jr. and L. O. Hocker, "Enhanced nonlinear optical affects in rotationally twinned crystals," Appl. Phys. Lett., 26, 442 (1975).
2. L. O. Hocker and C. F. Dewey, Jr., "Enhancement of second-harmonic generation in Zinc Selenide by crystal defects," Appl. Phys. Lett., 28, (1 March) (1976) (in press).

B. Periodic Phase Matching

1. J. A. Armstrong, N. Bloembergen, J. Ducuing, and P. S. Pershan, "Interactions between light waves in a nonlinear dielectric," Phys. Rev., 127, 1918 (1962).
2. R. C. Miller, "Optical harmonic generation in single crystal BaTiO_3 ," Phys. Rev., 134, A1313 (1964).
3. G. D. Boyd and C. K. N. Patel, "Enhancement of optical second-harmonic generation (SHG) by reflection phase matching in ZnS and GaAs," Appl. Phys. Lett., 8, 313 (1966).
4. S. Sonekh and A. Yariv, "Phase matching by periodic modulation of the nonlinear optical properties," Optics Comm., 6, 301 (1972).
5. Y. Yacoby, R. L. Aggarwal and B. Lax, "Phase matching by periodic variation of nonlinear coefficients," J. Appl. Phys., 44, 3180 (1973).
6. N. Bloembergen and A. J. Sievers, "Nonlinear optical properties of periodic laminar structures," Appl. Phys. Lett., 17, 483 (1970).

B. Periodic Phase Matching (continued)

7. J. D. McMullen, "Optical parametric interactions in isotropic materials using a phase-corrected stack of nonlinear dielectric plates," J. Appl. Phys., 46, 3076 (1975).
8. C. L. Tang and P. P. Bey, "Phase matching in second-harmonic generation using artificial periodic structures," IEEE J. Quant. Elec., QE-9, 9 (1973).
9. J. P. van der Ziel, "Phase-matched harmonic generation in a laminar structure with wave propagation in the plane of the layers," Appl. Phys. Lett., 26, 60 (1975).
10. N. Bloembergen, "Apparatus for converting light energy from one frequency to another," U. S. Patent 3,384,433, May 21, 1968.
11. W. E. Martin and D. B. Hall, "Optical waveguides by diffusion in II-VI compounds," Appl. Phys. Lett., 21, 325 (1972).

C. Growth and Twins in ZnSe, ZnTe, CdTe, and Hexamethylenetetramine

1. D. de Nobel, "Phase equilibria and semiconducting properties of cadmium telluride," Philips Res. Repts., 14, 361 (1959).
2. A. G. Fitzgerald, M. Manhami, E. H. Pogson and A. D. Yoffe, "Crystal growth and defect structure of zinc sulfide and zinc selenide platelets," J. Appl. Phys., 38, 3303 (1967).
3. D. E. Swets and E. S. Jorgensen, "The growth of hexamethylene-tetramine from solution and the vapor phase," J. Cryst. Growth, 5, 299 (1969).
4. P. Bomio, J. R. Bourne and R. J. Davey, "The growth and dissolution of hexamethylenetetramine in aqueous solution," J. Cryst. Growth, 30, 77 (1975).
5. W. P. Heim and K. A. Jones, "Calculations of the S_2 and Se_2 partial pressure and the ZnS-CdS and ZnSe-CdSe sublimation point diagrams," J. Electrochem. Soc., 122, 1739 (1975).
6. R. A. Duckett and A. R. Lang, "The growth of nearly perfect hexamethylenetetramine crystals from solution," J. Cryst. Growth, 18, 135 (1973).

C. Growth and Twins in ZnSe, ZnTe, CdTe, and Hexamethylentetramine (continued)

7. A. Libicky, "Synthesis and crystal growth of CdSe, ZnTe and ZnSe," Proc. 1967 Int. Conf. II-VI Semiconducting Components, D. G. Thomas, Ed., W. A. Benjamin, N. Y., 1967.
8. S. Vallette and Bernard Schaub, "Semi-conducteurs. Indices de refraction du tellurure de zinc (ZnTe)," C. R. Acad. Sc. Paris, 279, 33 (1974).
9. A. L. Fahrenbruch, V. Vasilchenko, F. Buch, K. Mitchell and R. H. Bube, "II-VI photovoltaic heterojunctions for solar energy conversion," Appl. Phys. Lett., 25, 605 (1974).
10. A. L. Gentile, J. E. Kiefer, N. R. Kyle and H. V. Winston, "A thermal annealing procedure for the reduction of $10.6 \mu\text{m}$ optical losses in CdTe," Mat. Res. Bull., 8, 523 (1973).
11. N. R. Kyle, "Growth of semi-insulating cadmium telluride," J. Electrochem. Soc., 118, 1791 (1971).
12. F. V. Wald and R. O. Bell, "Natural and forced convection during solution growth of CdTe by the traveling heater method (THM)," J. Cryst. Growth, 30, 29 (1975).
13. J. E. Kiefer and A. Yariv, "Electro-optic characteristics of CdTe at 3.39 and 10.6μ ," Appl. Phys. Lett., 15, 26 (1969).
14. J. M. Rowe, R. M. Nicklow, D. L. Price and K. Zanio, "Lattice dynamics of cadmium telluride," Phys. Rev., 10, 671 (1974).
15. W. Akutagawa and K. Zanio, "Vapor growth of cadmium telluride," J. Cryst. Growth, 11, 191 (1971).
16. H. Kimura and H. Komiya, "Melt compositions of II-VI compounds during crystal growth in a high-pressure furnace," J. Cryst. Growth, 20, 283 (1973).
17. T. B. Reed and W. J. Lafleur, "Dependence of growth temperature on carrier gas velocity in open tube transport," J. Cryst. Growth, 17, 123 (1972).
18. P. Blanconier and P. Henoc, "Croissance epitaxique de composés II-VI en phase vapeur," J. Cryst. Growth, 17, 218 (1972).
19. A. L. Gentile, N. R. Kyle and E. L. Kern, "Fabrication of ZnSe IR windows by physical vapor transport technique," Tech. Rept. AFML-TR-75-219, Hughes Research Laboratories, Malibu, Ca., January 1976.

C. Growth and Twins in ZnSe, ZnTe, CdTe, and Hexamethylentetramine (continued)

20. J. Steininger and A. L. Strauss, "Phase diagrams and crystal growth of pseudobinary alloy semiconductors," J. Cryst. Growth, 13/14, 657 (1972).
21. M. Rubenstein, "Solution growth of some II-VI compounds using tin as a solvent," J. Cryst. Growth, 3, 309 (1968).

D. Twinning Observed in Other Crystals

1. K. T. Aust and J. W. Rutter, "Some annealing phenomena in high-purity metals," in Ultra-High-Purity Metals, Am. Soc. Metals, Metals Park, Ohio, 1962, pp. 115-148.
2. J. F. Yee, M-C. Lin, K. Sarma and W. R. Wilcox, "The influence of gravity on crystal defect formation in InSb-GaSb alloys," J. Cryst. Growth, 30, 185 (1975).
3. H. M. Liaw and J. W. Faust, Jr., "Effect of growth parameters on habit and morphology of electrodeposited lead dendrites," J. Cryst. Growth, 18, 250 (1973).
4. H. J. Scheel and D. Elwell, "Surface features on flux-grown refractory oxide crystals," J. Cryst. Growth, 20, 259 (1973).
5. H. Matthes, A. Marshall, M. Gauntlett and J. Hesse, "Growth structure observations in czochralski-grown barium-lithium-niobate single crystals," J. Cryst. Growth, 26, 311 (1974).
6. K. J. Bachmann and E. Buehler, "The growth of La^3 crystals from the melt," J. Elect. Mat., 3, 279 (1974).
7. E. Kasper, H. J. Herzog and H. Kibbel, "A one-dimensional SiGe superlattice grown by UHV epitaxy," Appl. Phys., 8, 199 (1975).
8. D. Richman, in Compound Semiconductors, (R. K. Willerdson and H. L. Goering, Eds.), pp. 214 et seq., Reinhold Publ., N. Y., 1962.
9. R. S. Feigelson, R. K. Route and H. W. Swarts, "Solution growth of $CdGeAs_2$," J. Cryst. Growth, 28, 138 (1975).
10. R. K. Route, R. J. Raymakers and R. S. Feigelson, "Preparation of large untwinned single crystals of $AgGaS_2$," J. Cryst. Growth, 29, 125 (1975).

D. Twinning Observed in Other Crystals (continued)

11. D. C. Miller and A. F. Witt, "Analysis of growth related strain in czochralski grown indium antimonide using x-ray anomalous transmission topography," J. Cryst. Growth, 29, 19 (1975).
12. A. F. Witt and H. C. Gatos, "Impurity distribution in single crystals. II. Impurity striations in InSb as revealed by interference contrast microscopy," J. Electrochem. Soc., 113, 808 (1966).
13. N. Klausutis, J. A. Adamski, C. V. Collins, M. Hunt, H. Lipson, J. R. Weiner, "Growth of CdTe_{1-x}Se_x by the LEC and Bridgman technique," J. Elect. Matls., 1, 625 (1973).
14. K. J. Bachmann, L. Clark, Jr., E. Bushler, D. L. Malm and J. L. Shay, "Zone melting of indium phosphide," J. Electr. Matls., 4, 741 (1975).
15. K. J. Bachmann, E. Bushler, J. L. Shay, and A. R. Strnad, "Liquid encapsulated czochralski pulling of InP crystals," J. Elect. Matls., 4, 389 (1975).
16. P. H. Egli and L. R. Johnson, "Ionic Salts," in The Art and Science of Growing Crystals (J. J. Gilman, Ed.), Wiley, N. Y., 1963, esp. p. 212.
17. W. G. Burgers, "Principles of Recrystallization," ibid, esp. pp. 433-434.

E. Theory

1. J. W. Faust, Jr., and H. F. John, "The Growth of semiconductor crystals from solution using the twin-plane reentrant-edge mechanism," J. Phys. Chem. Solids, 25, 1407 (1964).
2. J. J. Gilman, Micromechanics of Flow in Solids, McGraw-Hill, N. Y., 1969.
3. R. L. Parker, "Crystal growth mechanisms: energetics, kinetics, and transport," in Solid State Physics: Advances in Research and Applications, 25 (H. Erenreich, F. Seitz, and D. Turnbull, Eds.), Academic Press, N. Y., 1970, pp. 151-299.
4. M. V. Klassen-Neklyndora, Mechanical Twinning of Crystals, Consultants Bureau, N. Y., 1964.

E. Theory (continued)

5. Y. Monfort, A. Maisseu, G. Allaie and A. Deschanvres, "Croissance orientee des sous oxydes de niobium dans la matrice," J. Cryst. Growth, 13/14, 829 (1972).
6. C. M. Sargent and V. S. Arunachalam, "Twining in superlattices," J. Scient. Ind. Res., 32, 555 (1973).
7. L. Däweritz, "Wahrscheinlichkeit der zwillingsbildung in dünnen schichten von Halbleitersubstanzen mit diamant-und zinkblendestruktur," Kristall und Technik, 7, 167 (1972).
8. R. A. M. Scott and L. W. Anson, "The origin of transverse striations in doped organic crystals," J. Cryst. Growth, 29, 147 (1975).
9. J. C. Brice, "Some thermodynamic aspects of the growth of strained crystals," J. Cryst. Growth, 28, 249 (1975).
10. N. Kobayashi, "Computational analysis of the flow in a crucible," J. Cryst. Growth, 30, 177 (1975).

APPENDIX VA

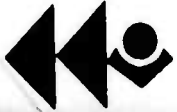
Nonlinear Optical Properties of $\bar{4}3m$ Crystals

INFORMATION SHEET

VI
properties of the II-VI crystals
CdS, CdSe, CdTe, ZnS, ZnSe, ZnTe

SEPTEMBER, 1975

	CdS	CdSe	CdTe	ZnS (Hex.)	ZnS (Cub.)	ZnSe	ZnTe
>50% Transmission for 2mm thickness (microns)	0.5 to 16	0.8 to 23 ⁽¹⁾	1 to 28		0.4 to 14	0.5 to 19	0.5 to >26
Absorption Coefficient at 10.6 microns (cm ⁻¹)	0.01	0.002	0.002			0.003	0.008
Indices of Refraction ⁽⁶⁾	1.50				2.420 ⁽⁵⁾		
n_0, n_g wavelengths in microns	0.56 2.566, 2.580 0.589 2.501, 2.519 0.60 2.404, 2.501 0.70 2.407, 2.424 0.75 2.386, 2.403 0.80 2.371, 2.387 1.00 2.330, 2.347 1.40 2.300, 2.316 3.39 2.4519, 2.4715 ⁽⁸⁾ 10.6 2.226, 2.239 ⁽²⁾		2.703, 2.710	2.356, 2.376 ⁽⁴⁾	2.369 ⁽⁴⁾ 2.3640 ⁽⁵⁾ 2.3333 ⁽⁵⁾	2.656 ⁽⁶⁾ 2.61 ⁽³⁾	3.054 ⁽⁹⁾ 3.035 ⁽⁹⁾ 2.913 ⁽⁹⁾ 2.879 ⁽⁹⁾ 2.863 ⁽⁹⁾ 2.790 ⁽⁹⁾ 2.741 ⁽⁹⁾ 2.70 ⁽⁸⁾
1/n dn/dT at 10.6 microns (10 ⁻⁶ /°C)			2.427, 2.447 ⁽¹⁾	2.66 ⁽³⁾ 42 ⁽¹³⁾		2.392 ⁽⁷⁾ 48 ⁽¹⁵⁾ , 38 ⁽⁷⁾	
Electro-Optic Constants				4.5 ⁽¹⁰⁾ , 8.8 ⁽⁸⁾ 44 ⁽¹³⁾	-1.1, -2.0 ^(11,12) 10.4 ⁽¹¹⁾	1.61 ⁽⁶⁾ , 2.0 ⁽⁸⁾ , 2.2 ⁽⁸⁾ 0.404, 0.546	4.51 ⁽⁹⁾ , 3.9 ⁽¹⁰⁾ 2.2 ⁽¹⁰⁾ , 7.1 ⁽¹⁰⁾ 0.589, 10.6
$r_{41} T (10^{-12} \text{m/V})$							
Half-wave Voltage (kV)							
Wavelength (microns)				1.0, 10.6			
$r_{41} S (10^{-12} \text{m/V})$							
Wavelength (microns)							
$r_{13} S (10^{-12} \text{m/V})$	1.1 ⁽⁸⁾	1.8 ⁽⁸⁾					
Wavelength (microns)	0.633	3.39					
$r_{33} S (10^{-12} \text{m/V})$	2.4 ⁽⁸⁾	4.3 ⁽⁸⁾					
Wavelength (microns)	0.633	3.39					
$r_c T (10^{-12} \text{m/V})$	4 ⁽³⁹⁾ , 5.5 ⁽⁸⁾						
Wavelength (microns)	0.589, 10.6						
Nonlinear Optical Susceptibilities							
(10 ⁻¹² m/V)							
(rounded off)							
at 10.6 microns ⁽⁸⁾	d ₁₄			-17 ± 6		31 ± 8	78 ± 29
	d ₃₃	44 ± 13	55 ± 13		37 ± 13		
	d ₃₁	-26 ± 6	29 ± 6		-19 ± 6		
	d ₁₅	29 ± 7	31 ± 8		21 ± 8		
et 1.06 microns ⁽⁸⁾	d ₃₆					25 ± 2	32 ± 2
	d ₁₄						3.0 ± 0.2
	d ₃₃	31 ± 2			15 ± 2		
	d ₃₁	-16 ± 1			-9 ± 2		
	d ₁₅	17 ± 1			8 ± 1		2.6 ± 0.3
Piezo-Optic Constants							
at 10.6 microns							
(10 ⁻¹² m ² /N)	a ₁₁				-5.91 ± 0.21 ⁽¹⁴⁾		
	a ₁₂				2.22 ± 0.08 ⁽¹⁴⁾		
	a ₄₄				-2.85 ± 0.33 ⁽¹⁴⁾		
Pulsed Damage Threshold			60				
(10 ⁸ W/cm ²)							
Crystal Structure ⁽¹⁶⁾	Hexagonal	Hexagonal	Cubic	Hexagonal	Cubic	Cubic	Cubic
	Wurtzite	Wurtzite	Sphalerite	Wurtzite	Sphalerite	Sphalerite	Sphalerite
Space Group ⁽¹⁶⁾	P6mc	P6mc	F43m	P6mc ⁽⁶⁾	F43m	F43m	F43m
Wurtzite Positional Parameter							
u ⁽¹⁷⁾ (ideal = 0.375)	0.378	0.377		0.374			
Lattice Constants (Å)	a_0	4.1367 ⁽¹⁸⁾ ± .0003	4.2972 ⁽¹⁸⁾ ± .0003	6.4830 ± .0004	3.8218 ⁽¹⁹⁾ ± .0004	5.4094 ⁽²⁰⁾ ± .0002	5.6687 ± .0002
at 25°C							
	c_0	0.7161 ± .0006	7.0085 ± .0006		6.25875 ± .0001		6.1034 ± .0003



CLEVELAND CRYSTALS, INC.

MAIL: Box 7157, Cleveland, Ohio 44117
PLANT: 19306 Redwood Avenue, Cleveland, Ohio 44110
TELEPHONE: (216) 486-6100

	CdS	CdSe	CdTe	ZnS (Hex.)	ZnS (Cub.)	ZnSe	ZnTe
Calculated Density, 25°C (g/cm ³)	4.619	5.670	5.849	4.067	4.080	5.262	5.636
Cleavage	[1120] [1010]	[1120] [1010]	[110]	[1120] [1010]	[110]	[110]	[110]
Thermal Expansion ^(c) (10 ⁻⁶ /°C) c	4.6 ₀	4.9 ₀	4.6 ⁽²¹⁾	6.6 ⁽²²⁾	5.9	7.1 ⁽⁷⁾	8.36
Temperature (°C)	29°-100°	29°-100°	50°	29°	26°-100°	29°	25°-100°
Thermal Conductivity, 25°C (W/cm/°C)	0.27		0.08			0.16	0.18
Specific Heat, 25°C (cal/g/°K)	0.088 ⁽²⁴⁾				0.116 ⁽²⁴⁾	0.016 ⁽²⁴⁾	
Melting Point (°C)	1397±2 ⁽¹⁸⁾	1258±2 ⁽¹⁶⁾	1097±2°	1718±16 ⁽²⁵⁾		1526±10 ⁽²⁵⁾	1292±5°
Vapor Pressure at M.P. (atm.)	2.1	0.81	1.5				0.6
Vapor Pressure (atm.): $\log_{10} P_T =$ (P _T -minimum total vapor pressure, T in °K)	-11.353 + 7.144	-11.101 + 6.948	-9.969 + 6.780		-12.778 + 6.830	-12.592 + 6.850	-11.101 + 6.981
Flexural Strength (psi)	~4000	~3000	~3000	~10,000		~8500	~3600
Estimated Maximum Safe Operating Temperature (°C)	>200°	>200°	>200°	>200°	>200°	>200°	>200°
Typical Dark Resistivity (ohm-cm)	>10 ⁸	>10 ⁸	10 ⁸		10 ⁹ -10 ¹⁰ (11)	10 ⁸ -10 ⁹ (23)	10 ⁸ -10 ⁹
Hall Mobilities (cm ² /V-sec)					100 ^(e)	400 ^(e)	130(h)
Highest measured at 300°K	350(e)	860(e)	1000 ^(e)			5000	2600
Highest measured at 80°K	5200	5000	10000			2.7	2.23 ⁽³²⁾
Energy Gap at 300°K (eV)	2.42 ⁽²⁸⁾	1.72 ⁽²⁹⁾	1.44 ⁽³¹⁾				-6.5x10 ⁻⁴ (32)
dE/dT (eV/°K)	-6 x 10 ⁻⁴ (27)	-4 x 10 ⁻⁴ (30)		3.6			
Effective Mass of Free Carriers							
Electrons	0.208m ₀ ⁽³³⁾	0.136m ₀	0.11m ₀	0.27m ₀		0.17m ₀	
Holes	2.1m ₀ ⁽³³⁾	0.7m ₀	0.63m ₀			0.6m ₀	
Sound Velocities, 25°C (m/sec)							
Longitudinal waves, Propagation and particle motion	c	4470	3980				
Propagation and particle motion	1c	4340	3610	3020	5080	4040	3580
Transverse waves, Propagation	[c]						
Particle motion	[1c]	1770	1520	1650	3380	2780	2350
Propagation	[1c]	1600	1530				
Propagation and particle motion	1c	1700 ⁽²⁸⁾	1600				
Dielectric Constants 25°C ⁽³⁴⁾	$\epsilon_{33} T/e_0$ 10.33	10.86			6.3 ₇	9.1 ₂	10.1 ₀
	$\epsilon_{11} T/e_0$ 9.36	9.70	11 ⁽¹³⁾				
	ϵ_{33}/e_0 9.53	10.20					
	ϵ_{11}/e_0 9.02	9.53					
Dielectric Constants, 25°C ⁽³⁴⁾	d_{31} -5.18	-3.92			8.3 ₂	9.1 ₂	10.1 ₀
$\times 10^{-12}$ Coul/Newton)	d_{33} +10.32	+7.84					
	d_{15} -12.98	-10.51					
	d_{14}		~1.5 ₄		3.1 ₈	1.1 ₀	0.9 ₁
(coul/m^2)	d_{31} -0.244	-0.160					
	d_{33} +0.440	+0.347					
	d_{15} -0.210	-0.138					
	d_{14}		~0.30 ₄		~0.14 ₇	0.04 ₉	0.028 ₄
Piezoelectric Coupling Factors ⁽³⁴⁾	k_{33} 0.262	0.194					
	k_{31} 0.119 ₁	0.083 ₆					
	k_{15} 0.188 ₅	0.130 ₅					
	k_1 0.154	0.124					
Elastic Constants ⁽³⁴⁾ (10 ⁻¹¹ m ² /N)	k_{14} 2.080	2.338			0.079 ₃	0.026	0.017
	k_{33} 1.697	1.736			1.839	2.26	2.40
	k_{12} -0.999	-1.122			-0.707	-0.15	-0.873
	k_{13} -0.881	-0.572					
	k_{44} 6.640	7.586			2.168	2.21	3.21
	k_{33} 6.136	6.920			~3.12 ₇ ⁽³⁶⁾		
	k_{11} 2.040	2.322			~1.10 ₇ ⁽³⁶⁾		
	k_{13} 1.581	1.870			~0.86 ₇ ⁽³⁶⁾		
	k_{12} -1.028	-1.138			~0.46 ⁽³⁶⁾		
	k_{13} -0.523	-0.539			~0.21 ⁽³⁶⁾		
	k_{44} 6.412	7.466			~3.51 ⁽³⁶⁾	2.154	2.27

	CdS	CdSe	CdTe	ZnS (Hex.)	ZnS (Cub.)	ZnSe	ZnTe
Elastic Constants ⁽³⁴⁾ (Continued)							
(10^{10} N/m ²)	c_{11}^E c_{33}^E c_{12}^E c_{13}^E c_{44}^E c_{66}^E c_{11}^D c_{33}^D c_{12}^D c_{13}^D c_{44}^D	9.07 9.38 5.81 5.10 1.504 1.630 9.13 9.623 5.88 4.97 1.560	7.41 8.36 4.52 3.93 1.317 1.445 7.42 6.477 4.83 3.86 1.340	5.351 ⁽³⁶⁾ 3.881 ⁽³⁶⁾ 1.994 ⁽³⁶⁾ ~3.2 ⁽³⁵⁾ ~12.4 ⁽³⁵⁾ ~14.0 ⁽³⁶⁾ ~8.0 ⁽³⁶⁾ ~4.5 ⁽³⁶⁾ ~2.86 ⁽⁷⁾	10.46 8.53 4.813 4.643	8.59 ⁽³⁷⁾ 5.06 ⁽³⁷⁾ 4.06 ⁽³⁷⁾ 8.59 ⁽³⁷⁾ 5.06 ⁽³⁷⁾ 4.06 ⁽³⁷⁾	

We have attempted to be as accurate as possible in gathering data and noting sources, but no guarantees can be made. In general, non-referenced material was internally generated, but it is possible that errors may appear. Apologies are offered to anyone whose data are miscredited. Any suggestions for corrections or additions will be incorporated into the next revision.

Mixed crystals are available in the systems CdS-CdSe with properties intermediate between the end members. Inquiries are welcomed.

FOOTNOTES

(a) Much of the data in the literature on the "hexagonal" form of ZnS is on polytypes that vary only slightly in bulk properties from the cubic form, although such is frequently not disclosed. We have attempted to evaluate the data on the internal evidence and to eliminate those which obviously do not apply to pure wurtzite. The attempt may not have been completely successful. Examples of information on polytypes may be found in the papers by I. B. Kobyakov, Soviet Phys. - Cryst. 11, 369-71 (1966) and Soviet Phys. - Solid State 9, 1269-71, 1707-11 (1967), and in reference 8. The data on the cubic form of ZnS are usually on material which is free of polytypes.

(b) References 21 and 3 give formulas for calculating indices of refraction versus wavelength

$$\text{For CdS: } n^2 = 5.235 + \frac{1.817 \times 10^7}{\lambda^2 - 1.651 \times 10^7} ; \quad n_0^2 = 5.239 + \frac{2.076 \times 10^7}{\lambda^2 - 1.651 \times 10^7}$$

$$\text{For ZnS: } n^2 = 5.164 + \frac{1.208 \times 10^7}{\lambda^2 - 0.732 \times 10^7}$$

$$\text{Or: } n^2 = A + \frac{B\lambda^2}{(\lambda^2 - C^2)} \text{ with } \begin{array}{lll} A & 5.08 & \text{CdTe} \\ B & 1.53 & \text{ZnSe} \\ C^2 & 0.366 & \text{ZnTe} \\ & & 0.113 \quad 0.142 \end{array}$$

(c.) Formulas for calculating thermal expansion versus temperature:

$$\text{CdS: } \frac{L_c}{L_0} = L = L_0 (1 + 4.0 \times 10^{-6}T + 11.5 \times 10^{-9}T^2 - 15 \times 10^{-12}T^3)$$

$$\frac{||c}{L_0} = L = L_0 (1 + 2.4 \times 10^{-5}T + 4.5 \times 10^{-9}T^2 - 5 \times 10^{-12}T^3)$$

$$\text{CdSe: } \frac{L_c}{L_0} = L = L_0 (1 + 4.6 \times 10^{-6}T + 3.0 \times 10^{-9}T^2)$$

$$\frac{||c}{L_0} = L = L_0 (1 + 2.8 \times 10^{-6}T + 2.0 \times 10^{-9}T^2)$$

$$\text{ZnTe: } L = L_0 (1 + 8.2 \times 10^{-6}T + 6.5 \times 10^{-9}T^2 - 5 \times 10^{-12}T^3)$$

$$L_0 = \text{Length at } 0^\circ\text{C, T is in } ^\circ\text{C}$$

$$\text{ZnSe}^{(38)}: a_t = 5.6681 \times 10^{-8} + 4.18 \times 10^{-13}t + 2.13 \times 10^{-18}t^2 + 2.79 \times 10^{-20}t^3$$

where a_t is the lattice constant in cm at t $^\circ\text{C}$.

REFERENCES

1. R. L. Herbst and R. L. Byer, Appl. Phys. Lett. 19, 527-30 (1971).
2. R. L. Byer, personal communication.
3. D. T. F. Marple, J. Appl. Phys. 35, 539-42 (1964).
4. C. Palache, H. Berman, and C. Frondel, *Handbook of Mineralogy* 7th Ed., Vol. 1, p. 211, 227, John Wiley and Sons, New York (1944).
5. W. L. Bond, J. Appl. Phys. 36, 1874-7 (1965).
6. R. W. McQuaid, Proc. IEEE 50, 2484-6 (1962); 51, 470 (1963).
7. J. R. Kurdock, Summary Report No. AFML TR-74-106, Part 1, Perkin Elmer Corp. (Oct., 1974).
8. R. J. Presley, Ed., *Handbook of Lasers*, Chapter 15 by I. P. Kaminow and E. H. Turner, p. 447-59 and Chapter 18, by S. Singh, p. 489-525, Chemical Rubber Publishing Co., Cleveland (1971).
9. T. R. Sticker and J. M. Jost, J. Opt. Soc. Am. 56, 130-1 (1966).
10. K. Tada and M. Aoki, Japen. J. Appl. Phys. 10, 998-1001 (1971).
11. S. Namba, J. Opt. Soc. Am. 51, 76-9 (1961).
12. C. K. N. Patel, Phys. Rev. Lett. 16, 813-18 (1966).
13. C.-C. Huang, Y.-H. Pao, P. C. Cleappy, and F. W. Phelps Jr., IEEE J. Quantum Electron 10, 186-91 (1974).
14. R. Wei and M. J. Sun, Proc. Int. Symp. CdTe, Mater. Gamma-Ray Detectors 1971, XIX 1-6 (1972).
15. C. S. Sahagian and C. A. Pitha, "Compendium on High Power Infrared Laser Window Materials", Special Report No. 135, Air Force Cambridge Research Labs, March 9, 1972.
16. J. D. H. Donnelly, et al., Editors, *Crystal Data*, 2nd Ed., ACA Monograph No. 5, Washington, D. C. (April 1, 1963).
17. Data calculated from the formula $\Delta u = 2/3 (a/c)^2 - 1/4$ given by G. A. Jeffrey, G. S. Parry, and R. L. Mozz, J. Chem. Phys. 25, 1024-31 (1951).
18. W. R. Cook Jr., J. Am. Ceram. Soc. 51, 518-20 (1968).

18. W. R. Cook Jr., *Nordica Reporter*.
20. B. J. Skinner and P. B. Barton Jr., *Am. Mineral.* **45**, 612-25 (1960).
21. W. L. Wolfe, Ed., *Handbook of Military Infrared Technology*, Superintendent of Documents, U. S. Govt. Printing Office, Washington, D. C. 20402
22. R. R. Reaber and G. W. Powell, *J. Appl. Phys.* **38**, 1531-4 (1967).
23. G. A. Zhukovich, *Soviet Phys. - Solid State* **2**, 1009 (1960).
24. A. J. Moses, *Optical Materials Properties*, IFI/Plenum, New York (1971).
25. L. A. Sysoev, et al., *Izv. Akad. Nauk SSSR* **3**, 390-1 (1967).
26. P. Goldfinger and M. Jouneshamma, *Mass Spectrometric and Knudsen-Cell Vaporization Studies of Group 2B-6B Compounds*, Aberdeen Press, Aberdeen (1963); Data modified by C.C.I. personnel.
27. C. C. Kick, *Phys. Rev.* **89**, 272 (1953).
28. M. Balkinovskii and R. D. Waldron, *Phys. Rev.* **112**, 123 (1958).
29. R. G. Wheeler and J. D. Dimmick, *Phys. Rev.* **125**, 1808 (1962).
30. R. H. Bulte, *Phys. Rev.* **98**, 431 (1956).
31. J. T. Milk, "Electro-optic Properties and Modulator Applications of Cadmium Telluride", Interim Report No. 75 (Revised), Air Force Materials Laboratory (Jan., 1971).
32. J. H. Heenstra and C. Heet, *Phys. Lett.* **2**, 21 (1962).
33. J. J. Heppfield and D. G. Thomas, *Phys. Rev.* **122**, 35-62 (1961).
34. D. Berlinecourt, H. Joffe, and L. R. Shiozawa, *Phys. Rev.* **129**, 1009-17 (1963). The value of 9.33 for $\epsilon_{11}^{\perp}/\epsilon_0$ in the paper was a misprint.
35. V. G. Zubov, L. A. Sysoev, and M. M. Firsova, *Soviet Phys.-Cryst.* **12**, 87-70 (1967).
36. H. J. McSkimin and D. G. Thomas, *J. Appl. Phys.* **35**, 2152-8 (1964).
37. B. H. Lee, *J. Appl. Phys.* **41**, 2983-90 (1970).
38. H. P. Singh and B. Doyal, *Phys. Status Solidi* **23**, K93-8 (1967).
39. D. J. A. Geron, *J. Opt. Soc. Am.* **54**, 270-1 (1964).

1.06 μ Doubling43_m - Td MATERIALS

Material	Transmission Range (μ)	Refractive Index n	Coherence Length 1.06 μ Doubling L_c (μ)	Nonlinear Coefficient $\times 10^{12}$ M _s D	Figure of Merit $\frac{D^2}{n^3} L_c^2$
$N_4(CH_2)_6$.3+2	1.6	17.	4.7	1500
CuI	.5+2.3	2.3	2.2	30	363
ZnS	.4+1.3	2.3	2.4	25	286
CuCl	.4+1.8	2.0	4.5	9.1	210
CuBr	.5+2.1	2.1	2.4	15	146
ZnSe	.5+2.1	2.6	1.5	32	123

$\overline{4}_3$ - Td MATERIALS

A-37

Material	Transmission Range	Refractive Index	Coherence Length 10μ Doubling L_f (μ)	Nonlinear Coefficient* $\times 10^{12}$ Mks D	Figure of Merit $\frac{D^2}{n^3} L_c^2$
CaSb	2 → 20μ (1	3.8 (5	134 (5	630 (5	130
CdTe	1 → 28 (3	2.7 (3	235 (8	86 (8	21
InAs	4 → 22 (1	3.5 (5	53 (5	420 (5	11.6
	1 → 17 (1	3.3 (5	104 (5	190 (5	10.9
GaAs	.6 → 25 (9	2.7 (2	290 (8	47 (8	9.4
ZnTe	.9 → 20 (6	3.5 (6	170** (6	170 (2	3.8
InP	.5 → 20 (7	2.2 (7	450 (7	11 (7	2.3
CuI	.5 → 22 (7	2.0 (7	370 (7	11 (7	2.1
CuBr					
ZnSe	.6 → 22 (3	2.5 (3	126 (8	40 (8	1.6
CaP	.6 → 12 (4	3.0 (5	46 (5	110 (5	0.95
AlSb	1.0 → 20 (6	3.3 (6	115** (6	50 (2	0.92
CuCl	.5 → 17 (7	1.9 (7	170 (7	9.5 (7	0.38

* Rel to GaAs Ref. 5 except for InP and AlSb.

** From index values.

References

- 1) McCarthy, App. Opt. 7, 1997 (1968).
- 2) Handbook of Lasers.
- 3) Handbook of Electronic Materials, Vol. 1
- 4) Kleinman and Spitzer, Phys. R. 118, 110 (1960).
- 5) J. J. Wynne and N. Bloembergen, Phys. Rev. 188, 1211 (1969).
- 6) R. K. Willardson and A. C. Beer, Semiconductors and Semimetals, Vol. 3, Academic Press.
- 7) D. Chemla et. al. Q.E. 7, 126 (1971).
- 8) C. K. N. Patel, Phys. Rev. Letts. 16, 613 (1966).
- 9) S. Narita and Al, J. Phys. Soc. Jap. 22, 1176 (1967).